Influence of nanocrystal size on optical properties of Si nanocrystals embedded in SiO2 synthesized by Si ion implantation

Tan, M. C.; Ding, Liang; Fung, Stevenson Hon Yuen; Liu, Yu Chan; Zhu, Fu Rong; Chen, Tupei; Liu, Yang; Yang, Ming; Wong, Jen It; Trigg, Alastair David

2007

Tan, M. C., Ding, L., Chen, T, P., Liu, Y., Yang, M., Wong, J. I., et al. (2007). Influence of nanocrystal size on optical properties of Si nanocrystals embedded in SiO2 synthesized by Si ion implantation. Journal of Applied Physics, 101, 1-6.

https://hdl.handle.net/10356/91752

https://doi.org/10.1063/1.2730560

Influence of nanocrystal size on optical properties of Si nanocrystals embedded in SiO_2 synthesized by Si ion implantation

L. Ding, T. P. Chen,[a] Y. Liu, M. Yang, and J. I. Wong
School of Electrical and Electronic Engineering, Nanyang Technological University, Singapore 639798, Singapore

Y. C. Liu
Singapore Institute of Manufacturing Technology, Singapore 638075, Singapore

A. D. Trigg
Institute of Microelectronics, Singapore 117685, Singapore

F. R. Zhu and M. C. Tan
Institute of Materials Research and Engineering, Singapore 117602, Singapore

S. Fung
Department of Physics, The University of Hong Kong, Hong Kong

(Received 3 December 2006; accepted 10 March 2007; published online 24 May 2007)

Si nanocrystals (nc-Si) with different sizes embedded in SiO_2 matrix have been synthesized with various recipes of Si ion implantation. The influence of nanocrystal size on optical properties, including dielectric functions and optical constants, of the nc-Si has been investigated with spectroscopic ellipsometry. The optical properties of the nc-Si are found to be well described by the four-term Forouhi-Bloomer model. A strong dependence of the dielectric functions and optical constants on the nc-Si size is observed. For the imaginary part of the dielectric functions, the magnitude of the main peaks at the transition energies E_1 and E_2 exhibits a large reduction and a significant redshift in E_2 depending on the nc-Si size. A band gap expansion is observed when the nc-Si size is reduced. The band gap expansion with the reduction of nc-Si size is in good agreement with the prediction of first-principles calculations based on quantum confinement. © *2007 American Institute of Physics*. [DOI: 10.1063/1.2730560]

I. INTRODUCTION

Over the past two decades, the emergence of the concept, silicon photonics, has greatly encouraged the intensive pursuit of inexpensive technologies for fabricating light emitters and modulators with Si-based materials.[1] Given that the Si light emitters, especially, lasers, are not commercially available, research in the field of Si photonics is still in an early stage. The most challenging step of Si photonics is to find a low-loss active medium that can be used for achieving optical gain and waveguiding in order to pave the way for fabricating a silicon laser in the wavelength of interest. However, bulk crystalline silicon is a poor light emitter at room temperature, mainly due to its low rate of radiative recombination as a result of its indirect band gap structure. During the 1990s, many different strategies were employed to overcome the problem. The most successful ones are based on the exploitation of low dimensional silicon in which the optical and electronic properties are modified by quantum confinement effects.[2–6] Silicon nanocrystals (nc-Si) are considered to be the preferable strategy for improving the light emission properties of silicon.[6]

SiO_2 thin film embedded with nc-Si, which is actually a planar waveguide, is considered as a very promising candidate for such an active medium with the advantages of chemical stability and full compatibility with the complementary metal oxide semiconductor (CMOS) process. Various techniques have been employed to synthesize nc-Si, including chemical vapor deposition (CVD),[7,8] sputtering,[9,10] pulse laser deposition (PLD),[11,12] and silicon ion implantation into SiO_2.[6,13–16] Among all these techniques, silicon ion implantation into a SiO_2 matrix followed by high temperature annealing is considered as one of the most promising methods for producing chemically and electrically stable nc-Si. It also allows for an accurate control of the depth distribution of nc-Si within the SiO_2 film and yields a smaller size (<10 nm) and a narrow size distribution of the nc-Si.

In such material system of SiO_2 matrix embedded with Si nanocrystals, the optical properties of isolated nc-Si should be different from those of bulk crystalline silicon due to the size effect, and should be also different from those of a continuous Si-nanocrystal film. Therefore, it would be interesting to examine the optical properties of isolated nc-Si embedded in SiO_2 matrix. Such a study is obviously important to the fundamental physics as it is concerned with a system of quantum dots isolated by a dielectric matrix, and it is also necessary to the optoelectronic and photonic applications of the nc-Si. Many investigations focusing on the theoretical calculations of optical properties of semiconductor nanocrystals using various methods such as empirical-pseudopotential approach and *ab initio* technique have been reported.[17–20] Some experimental studies on determining nc-Si optical properties have also been reported.[21–24] How-

[a]Electronic mail: echentp@ntu.edu.sg

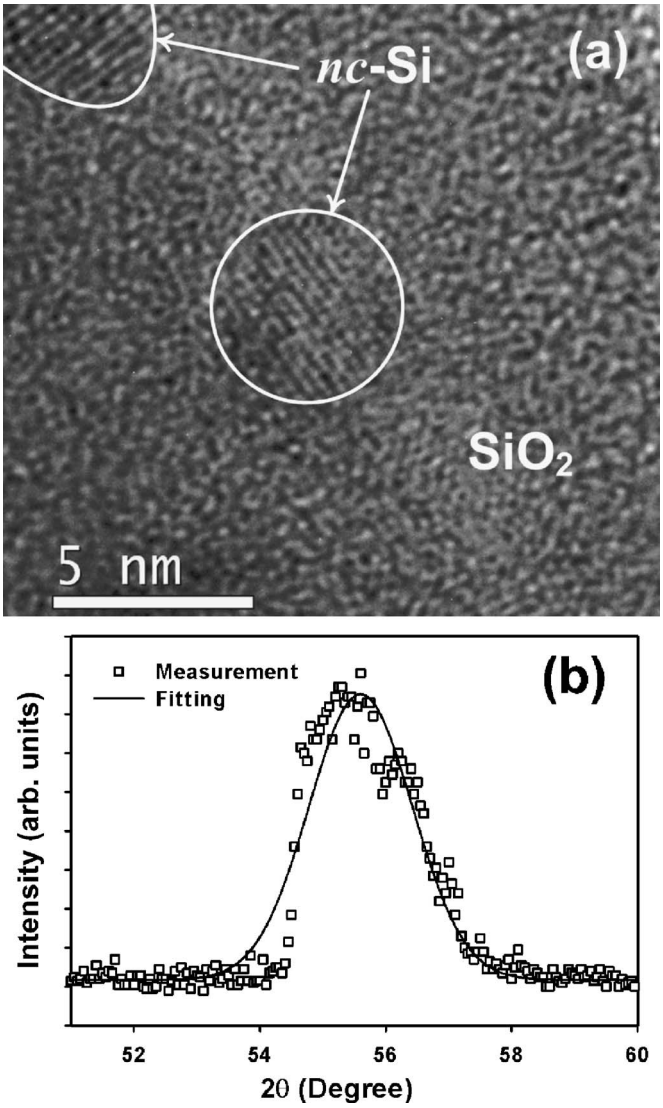

FIG. 1. HRTEM image (a) and XRD measurement (b) of nc-Si embedded in SiO_2 of sample 1.

ever, few experimental investigations on the size effect on optical properties of nc-Si embedded in SiO_2 matrix have been reported. In this work, the optical properties, including dielectric functions and optical constants, of nc-Si embedded in SiO_2 synthesized with Si ion implantation have been determined with spectroscopic ellipsometric (SE) analysis. The optical properties of nc-Si are modeled with the Forouhi-Bloomer (FB) formalism,[25] which can yield the energy band gap of the nc-Si. A large reduction in the dielectric functions and band gap expansion are found for the nc-Si, and a strong influence of nanocrystal size on the optical properties is observed.

II. EXPERIMENT

Wafers used in this study were *p*-type Si(100) with resistivity of 20–30 Ω cm. SiO_2 films with thickness of 550 nm were grown on the Si substrate by wet oxidation at 1000 °C. Afterwards, a high dosage of Si ions (10^{16}–10^{17} atoms/cm^2) were implanted into the SiO_2 films at various energies ranging from 100 to 3 keV (100, 50, 18, 5, and 3 keV) at room temperature, and the samples are denoted as samples 1–5, respectively. Implantations were conducted at 7° off axis to reduce channeling effect. Silicon nanocrystals were formed after high temperature annealing at 1000 °C for 20 min in N_2 ambient. As a typical example, Fig. 1(a) shows the high resolution transmission electron microscope (HRTEM) image of nc-Si embedded in SiO_2 matrix synthesized with Si^+ implantation at 100 keV (i.e., sample 1). The average size of nc-Si was determined from the broadening of Bragg peak in the x-ray diffraction (XRD) spectrum. As an example, Fig. 1(b) shows the XRD measurement for nc-Si embedded in SiO_2 matrix and the pseudo-Voigt fit to the data for sample 1. Table I gives the sizes of nc-Si for all the samples (i.e., samples 1–5) under the investigation in this study. SE measurement was carried out with a spectroscopic ellipsometer (J. A. Woollam Co., Inc.) in the wavelength range of 250–1100 nm with a step of 5 nm, and the incident angle was set at 75°.

TABLE I. Implantation energies and doses, maximum volume fractions of nc-Si in SiO_2, and the nc-Si sizes for the five samples.

Sample No.	Implantation energy (keV)	Dosage (ions/cm^2)	Peak volume fraction of nc-Si (%)	Size of nc-Si (nm)
1	100	1×10^{17}	17	4.6
2	50	8×10^{16}	28	5.3
3	18	5×10^{16}	40	5.8
4	5	5×10^{16}	60	6.3
5	3	5×10^{16}	93	7.6

III. METHODOLOGY

In this work, the band gap, dielectric functions and optical constants of the nc-Si are obtained from the SE analysis based on a multilayer model which is schematically shown in Fig. 2. The nc-Si depth distribution in the SiO_2 thin film is

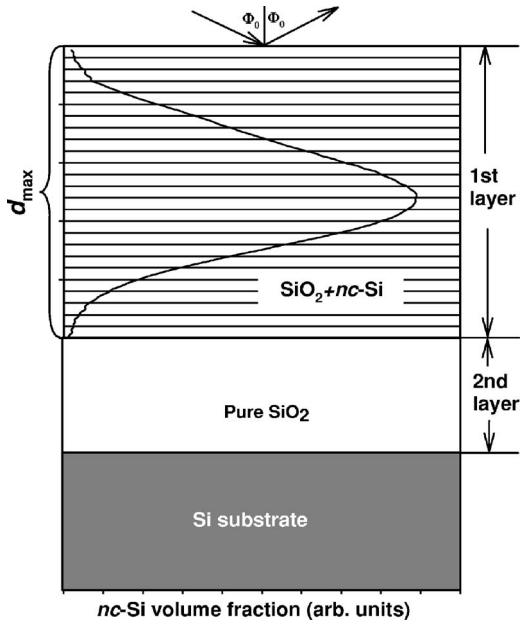

FIG. 2. The multilayer model used in the SE analysis. The curve schematically shows the distribution of the nc-Si in the SiO_2.

obtained from the stopping and range of ions in matter (SRIM) simulation. The SRIM intensity $I(x)$ due to the excess silicon in the Si^+-implanted region at a given depth x can be obtained by deducting the Si signal of the pure SiO_2 region from the total Si signal (which is from both the excess Si and the SiO_2) at the depth. The volume fraction of nc-Si at depth x should be proportional to the intensity $I(x)$. Thus the volume fraction $f(x)$ of the nc-Si embedded in SiO_2 at depth x can be expressed as

$$f(x) = \frac{QI(x)}{N_{\mathrm{Si}} \int_0^{d_{\max}} I(x)dx}, \tag{1}$$

where Q is the dose of implanted Si ions in the unit of atoms/cm^2, $d_{\max}$ is the maximum depth in SiO_2 beyond which no excess Si can be detected, and N_{Si} is the Si density in the unit of atoms/cm^3. In this study N_{Si} is equal to 5×10^{22} atoms/cm^3. It is found that the annealing after the ion implantation did not change the profile of excess Si in SiO_2 due to the low diffusion coefficient of Si in SiO_2 film. Thus, the $f(x)$ calculated with Eq. (1) represents the depth profile of the nc-Si volume fraction. Figure 3 shows the depth profiles of the volume fraction of nc-Si in SiO_2 for the five samples. The peak nc-Si volume fractions for the samples are also included in Table I.

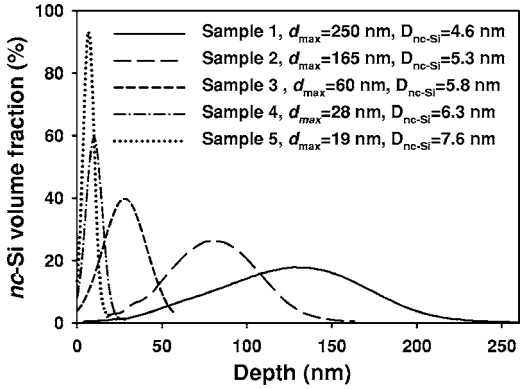

FIG. 3. Volume fractions of nc-Si in SiO_2 as a function of depth for the five samples obtained from SRIM simulation.

As shown in Fig. 2, the nc-Si distributes from the SiO_2 surface to a depth of $d_{\max}$, and almost no nc-Si can be found beyond $d_{\max}$. As such, the thin film was divided into two layers, namely, the first layer ($0 \leqslant \text{depth} \leqslant d_{\max}$) with nc-Si distributing in SiO_2, and the second layer ($\text{depth} > d_{\max}$) which is basically a pure SiO_2 without nc-Si. The thickness (d_1) of the first layer is equal to $d_{\max}$. The first layer is then further divided into n sublayers with equal thickness $d_0 = d_{\max}/n$ nm. Each sublayer can be optically schematized as an effective medium consisting of SiO_2 and the nc-Si, and its

TABLE II. Values of the parameters A_i, B_i, and C_i ($i=1,2,3,4$), $n(\infty)$, and E_g of the four-term FB model for the five samples. The corresponding values of bulk crystalline silicon are also included.

	nc-Si size (nm)	A_i	B_i (eV)	C_i (eV^2)	$n(\infty)$	E_g (eV)
Sample 1	4.6	0.0534	7.1121	12.7223	2.8143	1.7371
		0.0057	8.0148	16.0834	2.8143	
		0.0605	8.0312	18.7121	2.8143	
		0.0003	11.3674	33.6447	2.8143	
Sample 2	5.3	0.0458	7.1119	12.7176	2.8237	1.6864
		0.0089	8.0157	16.0797	2.8237	
		0.0843	8.3300	18.7101	2.8237	
		0.0113	10.3227	33.6447	2.8237	
Sample 3	5.8	0.0043	6.8850	11.8641	2.0179	1.6312
		0.0154	7.5102	14.1610	2.0179	
		0.0652	8.7143	19.1612	2.0179	
		0.1854	10.5212	29.2021	2.0179	
Sample 4	6.3	0.0145	7.0851	12.7275	2.0211	1.5312
		0.0146	7.4057	13.7881	2.0211	
		0.0653	8.7143	19.1601	2.0211	
		0.2154	10.5312	29.2021	2.0211	
Sample 5	7.8	0.0041	6.8854	11.8654	1.9498	1.4503
		0.0149	7.4013	13.7545	1.9498	
		0.0767	8.6341	18.8134	1.9498	
		0.2117	10.6517	29.8456	1.9498	
			Bulk crystalline silicon			
		0.0036	6.8811	11.8486	2.3688	1.12
		0.014	7.4013	13.7473	2.3688	
		0.0683	8.6348	18.7952	2.3688	
		0.0496	10.2339	26.5029	2.3688	

complex dielectric function can be calculated with an appropriate effective medium approximation (EMA).[26] In the SE analysis, the ellipsometric angles (Ψ and Δ) can be expressed as functions of the dielectric function ($\varepsilon_{\text{nc-Si}}$) of the nc-Si,[22] although these functions cannot be displayed with analytical formulas due to their complexity. A spectral fitting based on the functions to the experimental data of Ψ and Δ can yield the dielectric functions of nc-Si.[22] For the spectral fitting, an optical dispersion model is required. In the present work, the four-term FB model[22,25] was found to be the most suitable one to obtain a reasonable fitting in the photon energy range of 1–5 eV. Increase in the number of the FB model terms can improve the fitting. However, the improvement is not significant indicating that the four terms used in the FB model are the major contributors, while the computation time is increased significantly. The details of the four-term FB model can be found in Ref. 22. A spectral fitting to the experimental SE spectra yields the following parameters of the four-term FB model:[22] the parameters A_i, B_i and C_i (i=1, 2, 3, and 4) that are related to electron transition, the refractive index $n(\infty)$ for photon energy $E \rightarrow \infty$, and the energy band gap E_g of the nc-Si.

IV. RESULTS AND DISCUSSION

As can be seen in Table I, the size of nc-Si varies with the implantation recipe (i.e., the implantation energy and dose). This is actually a result of the variation in the concentration of excess Si in SiO_2. The excess Si with a higher concentration should tend to aggregate more easily and form nc-Si with a larger size during the high temperature annealing. As the concentration of excess Si in SiO_2 is determined by the implantation recipe (i.e, energy and dose), the nc-Si size can thus be varied in terms of the variation in the implantation energy and/or implantation dose. With this way we have been able to synthesize the five samples with various nc-Si sizes.

Using the methodology described in above section we have obtained the dielectric functions and optical constants of the nc-Si with various sizes embedded in SiO_2 for the five samples, and they are shown in Figs. 4 and 5, respectively. The dielectric functions and optical constants of bulk crystalline silicon are also included in the two figures for comparison. The parameters including A_i, B_i, C_i (i=1, 2, 3, and 4), $n(\infty)$, and E_g of the four-term FB model for the nc-Si with various sizes are given in Table II. For comparison, the corresponding parameters of bulk crystalline silicon are also included in the table.

As can be seen in Figs. 4 and 5, the nc-Si of all the samples exhibits a significant suppression in the dielectric functions and optical constants with respect to bulk crystalline silicon, and nc-Si size has a large influence on both the magnitude and shape of the spectra of the dielectric functions and optical constants. It is well known that dielectric functions of a crystalline material are closely associated with its electronic band structure which is often described by the joint density of states (DOS).[27] The critical points observed in the dielectric spectra of crystalline material are believed to originate from singularities in the joint DOS.[27] In Fig. 4, one can see that the imaginary part of the dielectric functions of bulk crystalline silicon show main peaks at the transition energies E_1(~3.4 eV) and E_2(~4.3 eV) as its critical points. The main peaks are responsible for the high absorption of the light wave by the material. As regard to the case of nc-Si embedded in SiO_2 as shown in Fig. 4(b), the magnitude of the imaginary part of the dielectric functions decreases when the nc-Si size is reduced. There is no much change in the transition energy of E_1 for all the samples, but a large redshift (~0.3 eV) in the transition energy of E_2 is observed for samples 1 and 2 which have a nc-Si size of 4.6 and 5.3 nm, respectively.

Table II clearly shows that the nc-Si exhibits a large expansion in the band gap as compared to that of the bulk crystalline silicon and the band gap of the nc-Si increases when the nc-Si size is reduced. For example, for the nc-Si with a size of 4.6 nm (sample 1), it has a band gap of 1.74 eV which is significantly larger than the band gap (1.1 eV) of the bulk crystalline silicon. The band gap expansion is the most direct evidence of quantum confinement effect of nc-Si. The band gap expansion of nc-Si and its dependence on the nanocrystal size have been demonstrated by some theoretical calculations of the band gap of nc-Si.[28,29] A fit to the first-principles calculation of the optical gap of silicon nanocrystal based on quantum confinement reported in Ref. 28 yields the band gap expansion (ΔE_g) as a function of nc-Si size as given below,

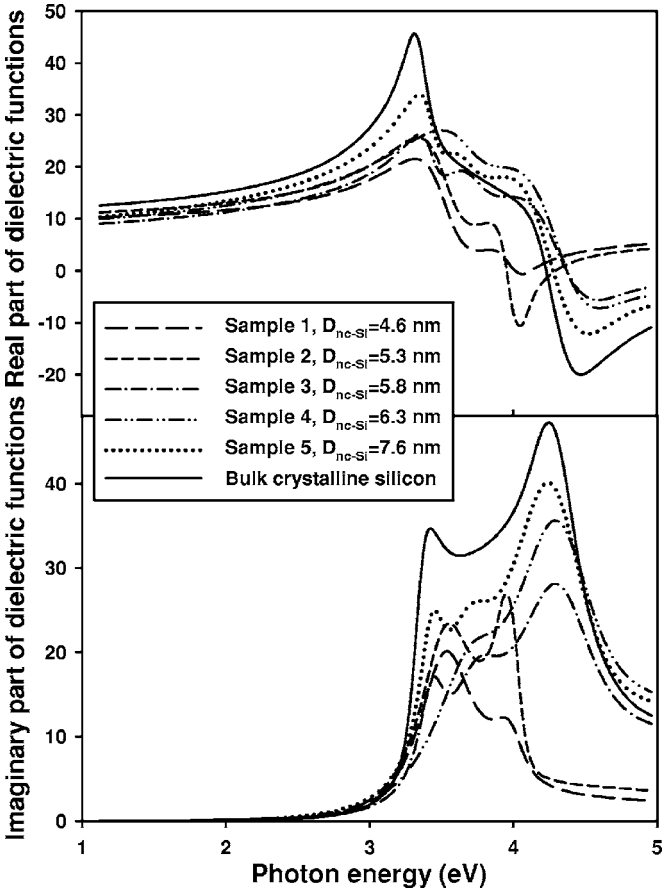

FIG. 4. Real (ε_1) and imaginary (ε_2) parts of the complex dielectric function of the nc-Si with various sizes obtained from the spectral fittings. The dielectric functions of bulk crystalline silicon are also included for comparison.

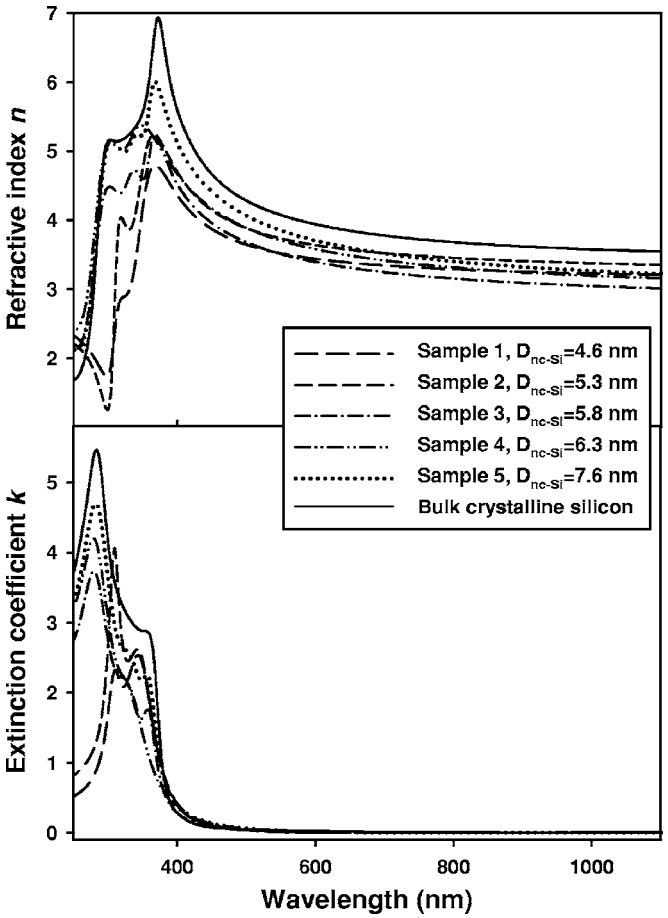

FIG. 5. Refractive index (n) and extinction coefficient (k) of the nc-Si with various sizes. The optical constants of bulk crystalline silicon are also included for comparison.

$$\Delta E_g(D) = E_g(D) - E_{g0} = C/D^n, \tag{2}$$

where D is the nc-Si size in nanometers, $E_g(D)$ is the band gap in eV of the nc-Si, E_{g0} is the band gap of bulk crystalline Si which is equal to 1.12 eV at room temperature, $C=3.9$, and $n=1.22$. A calculation of the band gap expansion with Eq. (2) is shown in Fig. 6, and the calculation is also compared with the band gap expansions obtained from the SE analysis discussed above. A good agreement in the comparison can be seen in Fig. 6. This suggests that the band gap expansion is due to the quantum confinement and thus the optical properties of the nc-Si observed in this study should be related to the quantum confinement also.

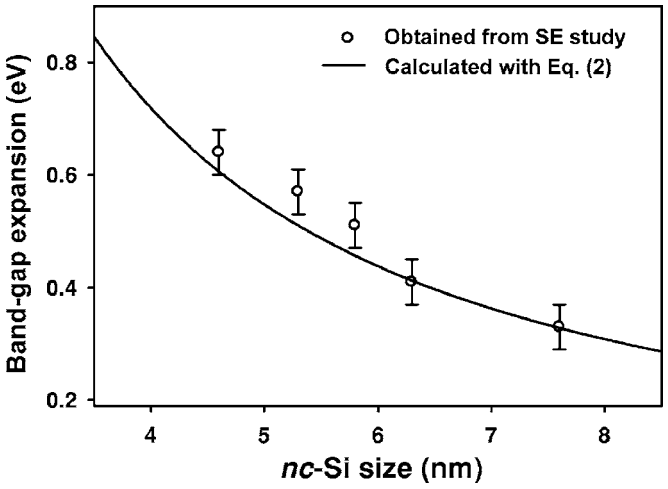

FIG. 6. Band gap expansion of nc-Si as a function of nc-Si size.

V. SUMMARY

Silicon nanocrystals with different sizes ranging from 4.6 to 7.8 nm embedded in SiO_2 have been synthesized with various implantation recipes (i.e., different implantation energies and doses). Optical properties, including the dielectric functions and optical constants, of the nc-Si have been studied in the photon energy range of 1.1–5 eV with spectroscopic ellipsometry based on the four-term Forouhi-Bloomer optical dispersion model. The band gap of the nc-Si embedded in SiO_2 is also obtained from the SE analysis. The influence of nanocrystal size on the optical properties of the nc-Si has been investigated. A strong dependence of the dielectric functions and optical constants on the nc-Si size is observed. For the imaginary part of the dielectric functions, the magnitude of the main peaks at the transition energies E_1 and E_2 exhibits a large reduction and a significant redshift in E_2 depending on the nc-Si size. A band gap expansion is observed when the nc-Si size is reduced. The band gap expansion with the reduction of nc-Si size is in good agreement with the prediction of first-principles calculations based on quantum confinement.

ACKNOWLEDGMENT

This work has been financially supported by the Ministry of Education, Singapore, under project ARC 1/04.

[1] M. Salib, L. Liao, R. Jones, M. Morse, A. Liu, D. Samara-Rubio, D. Aldunio, and M. Paniccia, Intel Technol. J. **8**, 143 (2004).
[2] L. T. Canham, Appl. Phys. Lett. **57**, 1046 (1990).
[3] A. G. Cullis and L. T. Canham, Nature (London) **353**, 335 (1991).
[4] W. L. Wilson, P. F. Szajowski, and L. E. Brus, Science **262**, 1242 (1993).
[5] K. D. Hirschman, L. Tsybeskov, S. P. Duttagupta, and P. M. Fauchet, Nature (London) **384**, 338 (1996).
[6] P. Mutti, G. Ghislotti, S. Bertoni, L. Bonoldi, G. F. Cerofolini, L. Meda, E. Grillo, and M. Guzzi, Appl. Phys. Lett. **66**, 851 (1994).
[7] J. F. Tong, H. L. Hsiao, and H. L. Hwang, Appl. Phys. Lett. **74**, 2316 (1999).
[8] N. M. Park, T. S. Kim, and S. J. Park, Appl. Phys. Lett. **78**, 2575 (2001).
[9] S. Furukawa and T. Miyasato, Jpn. J. Appl. Phys., Part 2 **27**, L2207 (1988).
[10] Q. Zhang, S. C. Bayliss, and R. A. Hutt, Appl. Phys. Lett. **66**, 1977 (1995).
[11] T. Yoshida, S. Takeyama, Y. Yamada, and K. Mutoh, Appl. Phys. Lett. **68**, 1772 (1996).
[12] X. Y. Chen, Y. F. Lu, Y. H. Wu, B. J. Cho, D. M. H. Liu, Y. Dai, and W. D. Song, J. Appl. Phys. **93**, 6311 (2003).
[13] H. M. Cheong, W. Paul, S. P. Withrow, J. G. Zhu, J. D. Budai, C. W. White, and D. M. Hembree, Appl. Phys. Lett. **68**, 87 (1996).
[14] S. Guha, M. D. Pace, D. N. Dunn, and I. L. Singer, Appl. Phys. Lett. **70**, 120 (1997).
[15] T. Komoda *et al.*, Nucl. Instrum. Methods Phys. Res. B **96**, 387 (1995).
[16] L. S. Liao, X. M. Bao, X. Q. Zheng, N. S. Li, and N. B. Min, Appl. Phys. Lett. **68**, 850 (1996).
[17] L. W. Wang and A. Zunger, Phys. Rev. Lett. **73**, 1039 (1994).
[18] C. Delerue, G. Allan, and M. Lannoo, Phys. Rev. B **48**, 11024 (1993).
[19] I. Vasiliev, S. Ogut, and J. R. Chelikowsky, Phys. Rev. Lett. **86**, 1813 (2001).
[20] H. C. Weissker, J. Furthmüller, and F. Bechstedt, Phys. Rev. B **67**, 165322

(2003).
[21]T. P. Chen, Y. Liu, M. S. Tse, O. K. Tan, P. F. Ho, K. Y. Liu, D. Gui, and A. L. K. Tan, Phys. Rev. B **68**, 153301 (2003).
[22]L. Ding, T. P. Chen, Y. Liu, C. Y. Ng, and S. Fung, Phys. Rev. B **72**, 125419 (2005).
[23]L. Ding, T. P. Chen, Y. Liu, C. Y. Ng, Y. C. Liu, and S. Fung, Appl. Phys. Lett. **87**, 121903 (2005).
[24]D. Amans, S. Callard, A. Gagnaire, J. Joseph, G. Ledoux, and F. Huisken, J. Appl. Phys. **93**, 4173 (2003).
[25]A. R. Forouhi and I. Bloomer, Phys. Rev. B **38**, 1865 (1988).
[26]R. M. A. Azzam and N. M. Basharra, *Ellipsometry and Polarized Light* (North-Holland, Amsterdam, 1977).
[27]S. Adachi, *Optical Properties of Crystalline and Amorphous Semiconductors: Materials and Fundamental Principles* (Kluwer Acdemic, Boston, 1999).
[28]S. Ogut, J. R. Chelikowsky, and S. G. Louie, Phys. Rev. Lett. **79**, 1770 (1997).
[29]L. W. Wang and A. Zunger, J. Phys. Chem. **98**, 2158 (1994).